
Diffusion Tensor Imaging: Introduction and Applications to Brain Tumor Characterization

2

Sumei Wang, Sungheon Kim, and Elias R. Melhem

Introduction

Brain tumors are the second leading cause of cancer-related deaths in children and adults younger than 39 years old, and they affect adults of all ages. The total number of newly diagnosed primary malignant or nonmalignant brain tumors was estimated to be 64,530 in 2004–2007, with 24,070 being malignant and 40,470 being nonmalignant, according to the Central Brain Tumor Registry of the United States (CBTRUS) [1]. Although the long-term survival of patients with brain tumors has been considerably improved over the last two or three decades, death still occurs in a significant proportion of the patients. In particular, glioblastoma, the most malignant primary brain tumor, presents a major challenge with a median survival time of only 12.2–18.2 months [2].

Brain tumor malignancy or grade is generally assessed according to World Health Organization (WHO) criteria, taking into account the cellularity, mitotic activity, endothelial proliferation, and necrosis [3]. Brain tumors consist of a variety of subtypes with a wide range of histopathology, molecular and genetic profile, clinical spectrum, and treatment options and outcome. The most common primary brain tumors in adults are glioblastomas and meningiomas. Brain metastases outnumber primary brain tumors in adults owing to high incidence of systemic cancer. Accurate diagnosis and grading of brain tumors are often crucial as the management and prognosis of different types of tumors are substantially different [4–6]. Pathological analysis of biopsy samples is the current gold standard for tumor grading. However, biopsy has limitations attributable to sampling error (e.g., missing the most malignant part) and is not always feasible (e.g., tumor in the brain stem).

Conventional MRI can display the anatomical appearance of brain tumor, but fails to provide physiologic and functional information that is crucial for tumor grading, predicting clinical outcome and response to therapy. Over the past few years, diffusion tensor imaging (DTI) has been increasingly used to study pathologic changes in brain tumors [7–10]. Various DTI metrics can be derived from the imaging data to provide information about the orientation and architecture of tissue microstructure at the voxel level. In this chapter, we briefly explain the DTI technique, followed by application of various DTI metrics in brain tumor characterization.

S. Wang, M.D. (✉)

Division of Neuroradiology, Department
of Radiology, Hospital of the University
of Pennsylvania, 219 Dulles Building, 3400 Spruce
St., Philadelphia, PA 19104, USA
e-mail: Sumei.Wang@uphs.upenn.edu

S. Kim, Ph.D.

Department of Radiology, Center for Biomedical
Imaging, New York University School of Medicine,
New York, NY 10016, USA

E.R. Melhem, M.D., Ph.D.

Department of Diagnostic Radiology and Nuclear
Medicine, University of Maryland School of
Medicine, Baltimore, MD 21201, USA

Basic Principles of Diffusion Tensor Imaging

Water molecules, the principle components of the brain, are in constant motion caused by random thermal fluctuation. By applying a pair of dephasing and rephrasing magnetic field gradients, MR imaging may be sensitized to the motion (diffusion) in the direction of the field gradient. This gradient pulse configuration is often known as diffusion weighting [11]. The degree of diffusion weighting is described by the b value, a parameter that is determined by the amplitude and timing of diffusion gradients. The measurement of signal loss or attenuation is a function of the diffusivity in a chosen direction as shown below:

$$S = S_0 e^{-bD} \quad (2.1)$$

where S is the diffusion-weighted signal, S_0 is the signal without diffusion weighting, and D is the estimated diffusivity or apparent diffusion coefficient (ADC). Acquiring diffusion-weighted images with at least two different b values allows the determination of the diffusivity for each image voxel.

In white matter, diffusion is anisotropic, as axonal membranes and myelin sheaths restrict and/or hinder this molecular motion in a particular direction. Apparent diffusivity of water is generally higher in directions parallel to fiber tracts than in the perpendicular direction [12]. Three-dimensional probability distribution of diffusivity can be described by a diffusion tensor ellipsoid with three eigenvectors and the corresponding eigenvalues (λ_1 , λ_2 , and λ_3). The eigenvector associated with the largest eigenvalue denotes the predominant orientation of fibers in a given imaging voxel. If a particular voxel has a high degree of anisotropy, one of the eigenvalues will be much higher than the other two.

Most commonly used indices for diffusion tensor are mean diffusivity (MD) and fractional anisotropy (FA) [13], which can be calculated according to (2.2) and (2.3), respectively:

$$MD = (\lambda_1 + \lambda_2 + \lambda_3) / 3 \quad (2.2)$$

$$FA = \sqrt{\frac{3}{2}} \sqrt{\frac{(\lambda_1 - \bar{\lambda})^2 + (\lambda_2 - \bar{\lambda})^2 + (\lambda_3 - \bar{\lambda})^2}{\lambda_1^2 + \lambda_2^2 + \lambda_3^2}} \quad (2.3)$$

where $\bar{\lambda}$ denotes mean of the three eigenvalues. MD is a measure of the directionally averaged magnitude of diffusion and is related to cell density, size, and parenchyma permeability. FA represents the degree of diffusion anisotropy, and reflects the degree of alignment of cellular structure [13].

Although FA is a good indicator of diffusion anisotropy, it does not provide information on the shape of the diffusion ellipsoid. For example, it cannot distinguish a flat ellipsoid from an oblong one. Westin et al. [14] have modeled diffusion anisotropy using a set of three basic metrics that depend on the shape of the diffusion tensor: linear anisotropy coefficient (CL) where diffusion is mainly along the direction corresponding to the largest eigenvalue; planar anisotropy coefficient (CP) where diffusion is mainly restricted to the plane spanned by the two eigenvectors with the two largest eigenvalues; and spherical anisotropy coefficient (CS), which indicates isotropic diffusion. The CL, CP, and CS values can be calculated using the following equations:

$$CL = (\lambda_1 - \lambda_2) / (\lambda_1 + \lambda_2 + \lambda_3) \quad (2.4)$$

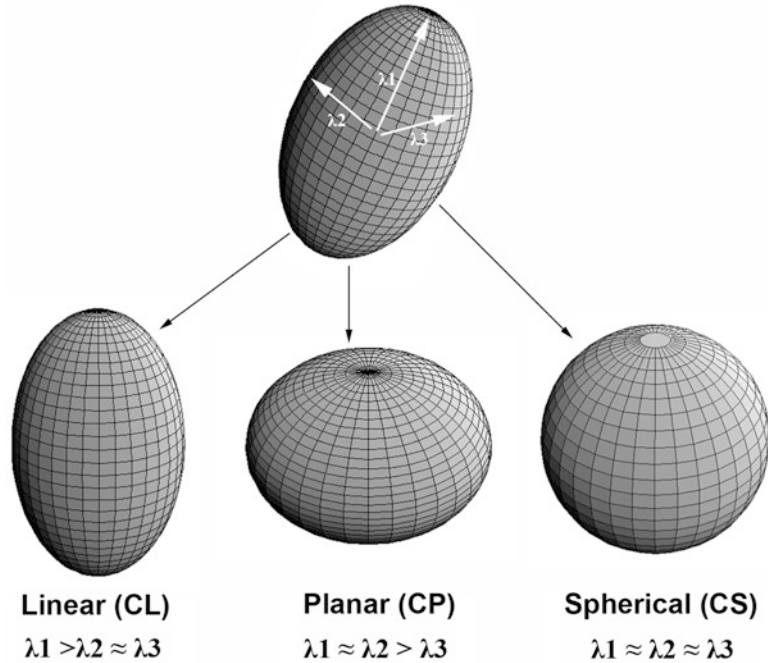
$$CP = 2(\lambda_2 - \lambda_3) / (\lambda_1 + \lambda_2 + \lambda_3) \quad (2.5)$$

$$CS = 3\lambda_3 / (\lambda_1 + \lambda_2 + \lambda_3) \quad (2.6)$$

The CL, CP, and CS values lie in the range from 0 to 1 and the sum of these three metrics is equal to 1 (Fig. 2.1).

Each anisotropy measure shows unique features in different regions of white matter. These differences arise from the relative contribution of the linear, planar, and spherical shape components of the diffusion tensor. Linear ellipsoid is typically found in regions with parallel arrangement, such as corpus callosum and pyramidal tract. Planar ellipsoid corresponds to regions of fibers with different orientations, or bundles of fibers that are randomly oriented in a plane, such as centrum semiovale and subcortical white matter regions. The gray matter appears isotropic with high CS [15]. These studies suggest that tensor shape measurements allow one to explore the tissue microstructural difference.

Fig. 2.1 Three shapes of diffusion ellipsoid



Application to Brain Tumor Characterization

Water diffusion is affected by tissue constituents, such as macromolecules, membranes, and organelles, as well as by tissue microstructure and organization. From the metrics derived from DTI, one can infer information about the brain tissue that cannot be obtained using conventional MRI. In brain tumors, microstructural tissue characteristics vary significantly between tumor types, including the cellularity, presence of tumor necrosis, fibrous tissue within tumors, tumor infiltration, and so forth. DTI is a promising tool for detecting such microscopic difference in tumors.

Most of DTI studies in brain tumors focused on the analysis of different parts within the tumor using various DTI metrics. But it is often helpful to measure reactive and infiltrative changes in the tissue surrounding the tumor. The neoplastic mass can be generally subdivided into two regions: the solid part of the tumor and central necrotic or cystic part of the tumor. Similarly, the peritumoral edematous region can be separated into two regions: proximal region surrounding

the enhancing part of the tumor potentially including infiltrative tumor cells, and more distal region mainly comprising vasogenic edema. These four subregions of a neoplasm can be substantially different from each other in terms of their DTI metrics. A variety of methods to analyze diffusion information have been proposed and range from simple mean/median value to histogram analysis over the selected regions of interest (ROIs). Systematic analysis of various DTI metrics including tensor shape measures from these different areas may provide a robust way for characterization of brain neoplasms.

Mean Diffusivity and Tumor Cellularity

Of all the histologic features used in tumor classification, cellularity has been the main target of assessment with DTI. MD measures the magnitude of diffusion within cerebral tissues. The higher the tumor cellularity, the lower the MD value due to decrease in the extracellular space (i.e., increased hindrance to extracellular water diffusion, assuming that the intracellular water

diffusion is restricted) [12, 16]. This inverse correlation between MD and cellularity has been reported in both glial [9] and nonglial tumors [17].

MD values have been used in differentiating tumor grades [7, 8, 18, 19] and types [8, 20–22], however, with mixed results. Some reports have suggested that mean MD [20, 23, 24], minimum MD [7] [25], or MD ratio [18, 19] is helpful for grading and tumor differentiation, while others indicated the limited use of MD in the differentiation of neoplasms [8, 26–28]. Those studies in which MD was found useful have generally observed lower diffusivities in high-grade or more cellular tumors. It has been accepted that primary cerebral lymphomas and medulloblastomas have lower MD values because of densely packed cells in these tumors [8, 17]. Also atypical or malignant meningiomas were found to have lower MD values compared with typical meningiomas [18, 19, 29]. However, MD itself is very limited in ++ tumor classification with low sensitivity and specificity [21, 22]. Besides cellularity, other factors such as extracellular matrix, viscosity, and mucins may also affect the measurement of MD [30, 31].

MD has also been used to monitor tumor treatment response. In most malignant tumors, successful treatment is reflected by increases in MD values. This may be due to the cellular death and vascular changes in response to treatment. Results from animal models [32] and clinical studies [33] provide supportive evidence for the use of MD as a responsive biomarker. A novel method called functional diffusion mapping (fDM) has been introduced to map voxel-by-voxel changes of apparent diffusivity over time [2, 34].

Diffusion Anisotropy of Tumor

FA is the most commonly used anisotropy index. FA reflects the degree of alignment of tissue microstructure, and as such its use may not be limited to the white matter tracts alone [12]. Regions of relatively high anisotropy have been reported in brain abscesses [35], glioblastomas [36, 37], and areas of hemorrhage [38], indicating that the tissues other than the white matter can also have preferentially oriented structures.

In contrast to MD, the relationship between FA and tumor cellularity is unclear, as both positive [36, 37, 39] and negative [9, 40] correlation has been reported. While Inoue et al. [41] stated that FA values of low-grade gliomas were significantly lower than those of high-grade gliomas, Stadlbauer et al. [9] reported lower FA values in high-grade gliomas. A recent study reported that mean and maximal FA from the solid part of the tumor are useful in grading non-enhancing gliomas [26]. For tumor type differentiation, Wang W et al. [42] and Reiche et al. [43] reported lower FA from the enhancing regions of glioblastomas compared with brain metastases, whereas Wang S et al. [22] observed higher FA in the enhancing regions of glioblastomas than in those of metastases. One likely reason for these contradictory results is the lack of standardized methods, both for acquisition as well as postprocessing and selection of ROI. It has also been demonstrated by Wang et al. [21] that FA in glioblastomas is higher than that in both brain metastases and primary cerebral lymphomas (Figs. 2.2, 2.3, 2.4, and 2.5). Among these three tumor types, lymphomas have the highest cellularity, followed by glioblastomas and brain metastases [44–46]. These findings indicate that diffusion anisotropy may not directly correlate with tumor cellularity. It has been reported that FA of tumor can be affected by several factors including extracellular-to-intracellular space ratio, extracellular matrix, tortuosity, and vascularity [30, 31]. Further study is warranted to help understand the underlying tumor microstructure contributing to FA.

Shape-Based Diffusion Tensor Metrics

Information on the geometric nature of diffusion tensor provides further differentiation of tumor types based on tensor shape in addition to FA [14, 15, 47]. Both CL and CP values contribute to FA observed in tissue and their relative values indicate the shape of diffusion ellipsoid [15]. Anisotropy changes within and surrounding the tumor have been demonstrated in animal studies, indicating that tensor shape is related to the macroscopic organization of tumor cells [48–50].

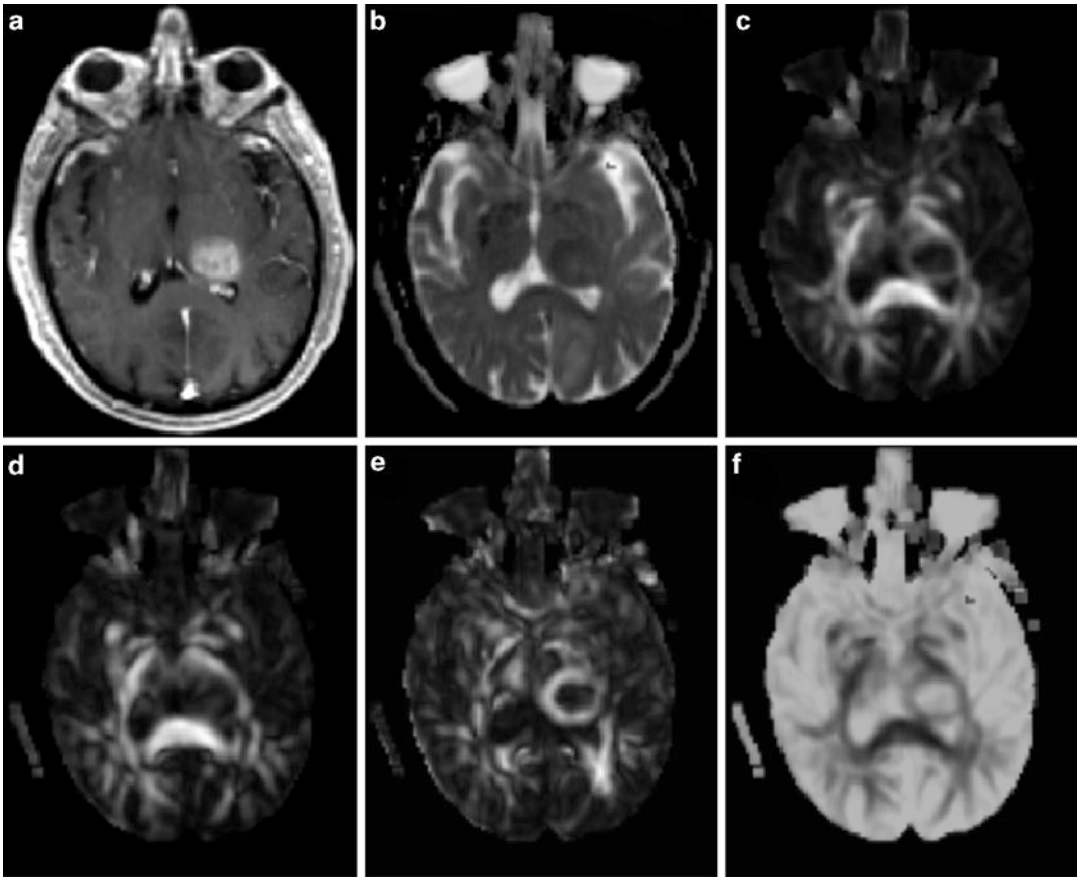


Fig. 2.2 A 71-year-old male with a glioblastoma in the *left* thalamus. Axial contrast-enhanced T1-weighted image (a) shows solid enhancement. MD map (b) shows restricted diffusion of the enhancing part ($0.75 \times 10^{-3} \text{mm}^2/\text{s}$). FA (c), CL (d), and CP (e) from the enhancing part (0.18, 0.15, and

0.15, respectively) are higher than those for brain metastasis (Fig. 2.3) and primary cerebral lymphoma (PCL, Fig. 2.4). CS (f) from the enhancing portion (0.68) is lower compared with brain metastasis and PCL. Reprinted and modified with permission from Wang et al. [21]

The types of the tumor, the degree of invasiveness, and growth rate can affect the diffusion properties [49, 50]. Tensor shape measurements have also been used to characterize pathologic changes in the human brain. Zhang et al. [47] reported lower CL in brain metastases than in contralateral normal brain. Elevated FA and CP along with decreased CS were observed in fibroblastic meningiomas compared with other subtypes of meningiomas [29, 51, 52]. Kumar et al. [53] reported high CP and low CL in the abscess cavity compared with normal white matter, thus distinguishing true from pseudo white matter tracts. It has also been reported that epidermoid cysts have high CP [54] and tuberculomas showed

lower CL, CP, and higher CS [55] compared with normal white matter. Wang et al. [21] also demonstrated higher FA, CL, and CP from the enhancing part of glioblastomas in comparison to both brain metastases and primary cerebral lymphomas (Figs. 2.2, 2.3, 2.4, and 2.5). These results suggest that tensor shape measurements provide additional information about tissue characteristics, which may further aid in tumor classification.

A ring with high CP has been reported in glioblastomas, brain metastases, and meningiomas. While the potential reason for the observation of this ring remains speculative, its presence may reflect compression of surrounding tissue by the tumor [47, 52].

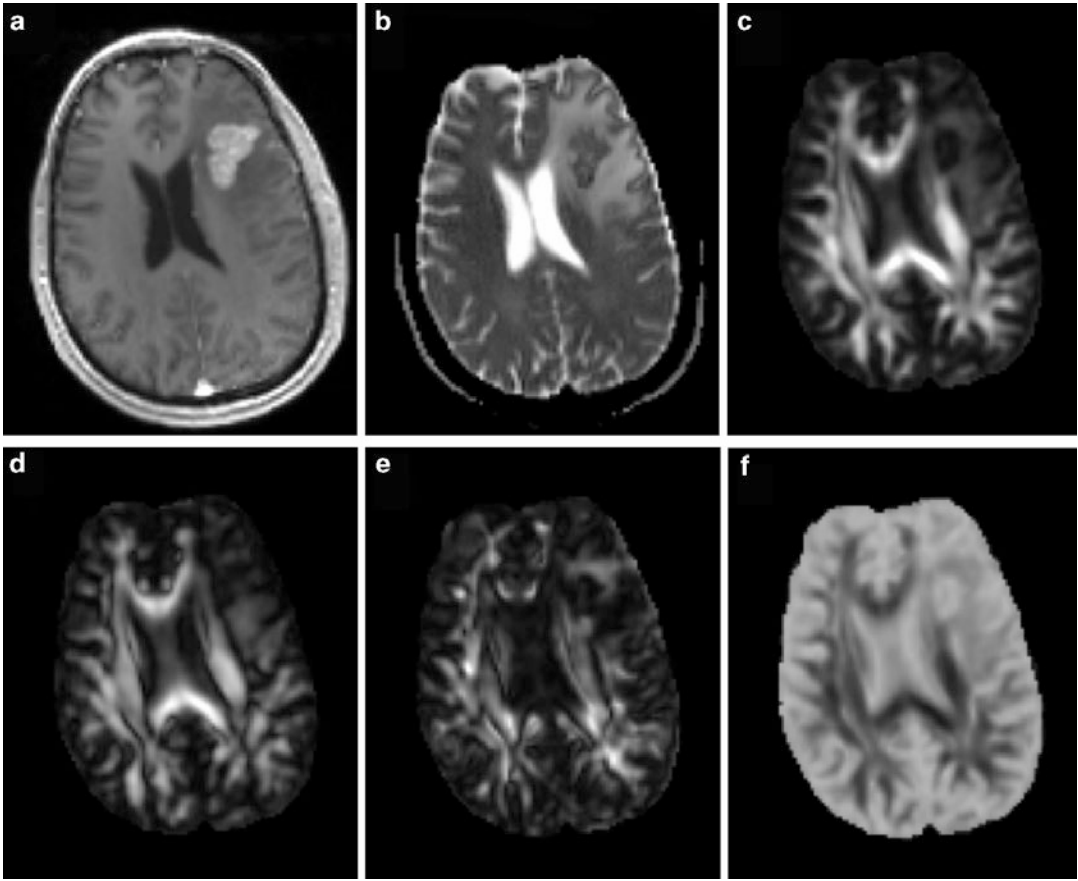


Fig. 2.3 A 53-year-old male with metastatic lung adenocarcinoma in the *left* frontal lobe. Axial contrast-enhanced T1-weighted (a) shows a solid enhancing lesion. MD map (b) shows restricted diffusion of the enhancing part ($0.95 \times 10^{-3}/\text{mm}^2/\text{s}$). Lower FA (c), CL (d), and CP (e) are

noticed from the enhancing part (0.10, 0.08, and 0.09, respectively) relative to normal-appearing white matter compared with the glioblastoma. CS (f) appearance looks similar to glioblastoma (Fig. 2.2f), but has a higher value (0.82)

DTI and Tumor Infiltration

Peritumoral region is usually defined as the area of abnormality surrounding the enhancing part of the tumor. In metastatic brain tumors or noninfiltrative primary tumors such as meningiomas, peritumoral edema is widely regarded as vasogenic edema. In this region, increased extracellular water is present due to leakage of plasma from altered tumor capillaries. Also this region does not include any tumor cells. In gliomas, however, the peritumoral region includes both vasogenic edema and infiltrating tumor cells.

Investigators have tried to use DTI to differentiate tumor-infiltrated edema from pure vasogenic edema [20, 22, 24], which may be beneficial for

accurate preoperative diagnosis of glioblastomas and metastases. Lu et al. [20] reported a significant difference between tumor-infiltrated edema and pure vasogenic edema using a parameter called “tumor infiltration index,” which measures departure from a linear relationship between MD and FA. These authors also reported higher MD in metastasis compared to glioblastomas. However, other studies demonstrated lower MD and minimum MD or MD ratio in the peritumoral region of metastases compared to that of glioblastomas [24, 56]. In contrast, van Westen et al. [57] reported no difference in MD and FA values in the peritumoral region of glioblastomas, metastases, and meningiomas. Recently, Kinoshita et al. [58] claimed that “tumor infiltration index” could

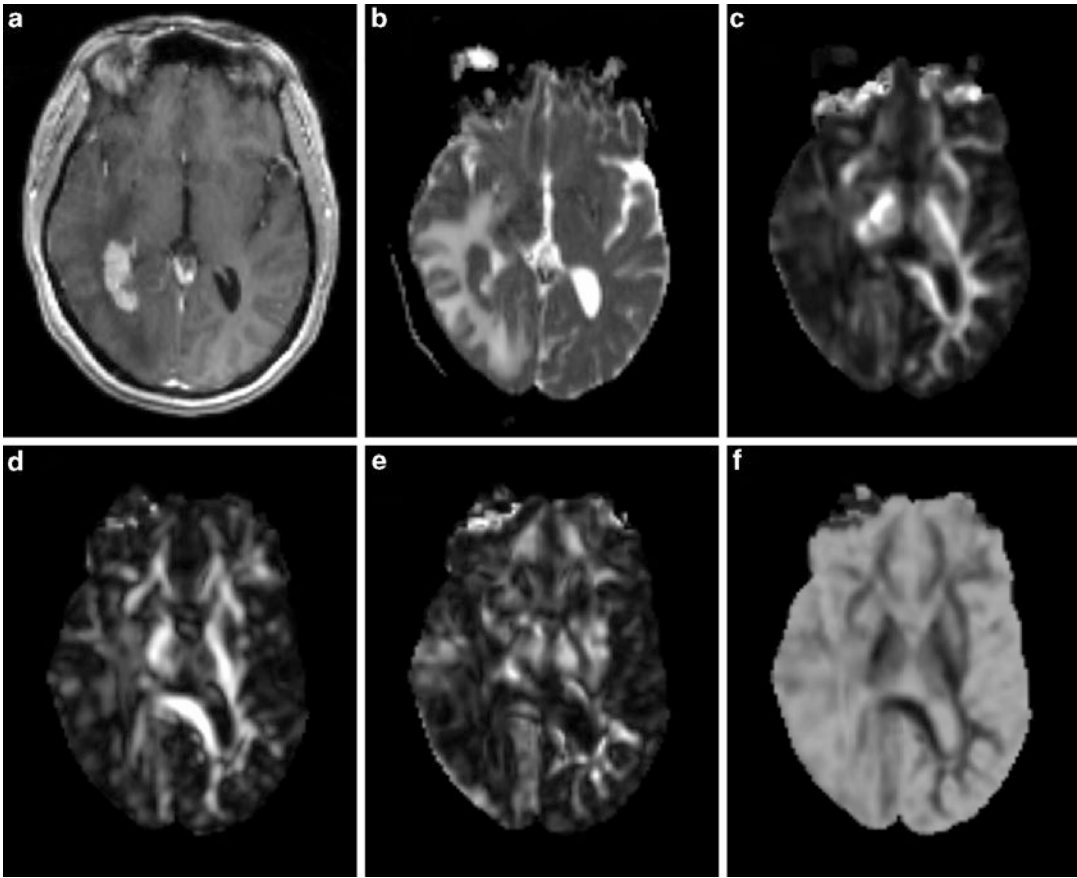


Fig. 2.4 A 58-year-old female with primary cerebral diffuse large B cell lymphoma in the *right* peritrigonal area. Axial contrast-enhanced T1-weighted (a) shows a solid enhancing lesion with extensive edema. MD map (b) shows restricted diffusion of the enhancing part (0.80×10^{-3} /

mm^2/s). Lower FA (c), CL (d), and CP (e) are noticed from the enhancing part (0.08, 0.08, and 0.06, respectively) relative to normal-appearing white matter compared with the glioblastoma. CS (f) from the enhancing part appears higher (0.85) compared with glioblastoma

not differentiate vasogenic edema from tumor-infiltrated edema. The difference in defining the ROIs for the peritumoral region in these studies may in part be responsible for the discrepancy. A number of studies have focused on the area close to the enhancing region (peritumoral region) either by manually placing a number of small ROIs around the tumor [23, 24] or by using a band of arbitrarily chosen thickness around the tumor [28, 59]. In the study reported by Wang et al. [22], the peritumoral areas were further subdivided into immediate peritumoral region and distant peritumoral region with the hypothesis that the immediate peritumoral region may have a higher degree of tumor infiltration in glioblastomas. There was a significant difference in FA,

CL, and CP between glioblastomas and metastases in the immediate peritumoral region. In the distant peritumoral region, only FA and CP measurements reached significant difference between the two tumor types [22]. While statistical significance was observed, the overall sensitivity, specificity, and accuracy for all the DTI metrics in the peritumoral areas were lower than in the enhancing part of the tumor. Since the edematous region contains areas of increased extracellular water, tumor infiltration, and varying fractional composition of normal white/gray matter, it is difficult to determine which factor dominates the DTI metrics. These confounding factors may further explain the conflicting reports of DTI characteristics in the peritumoral regions.

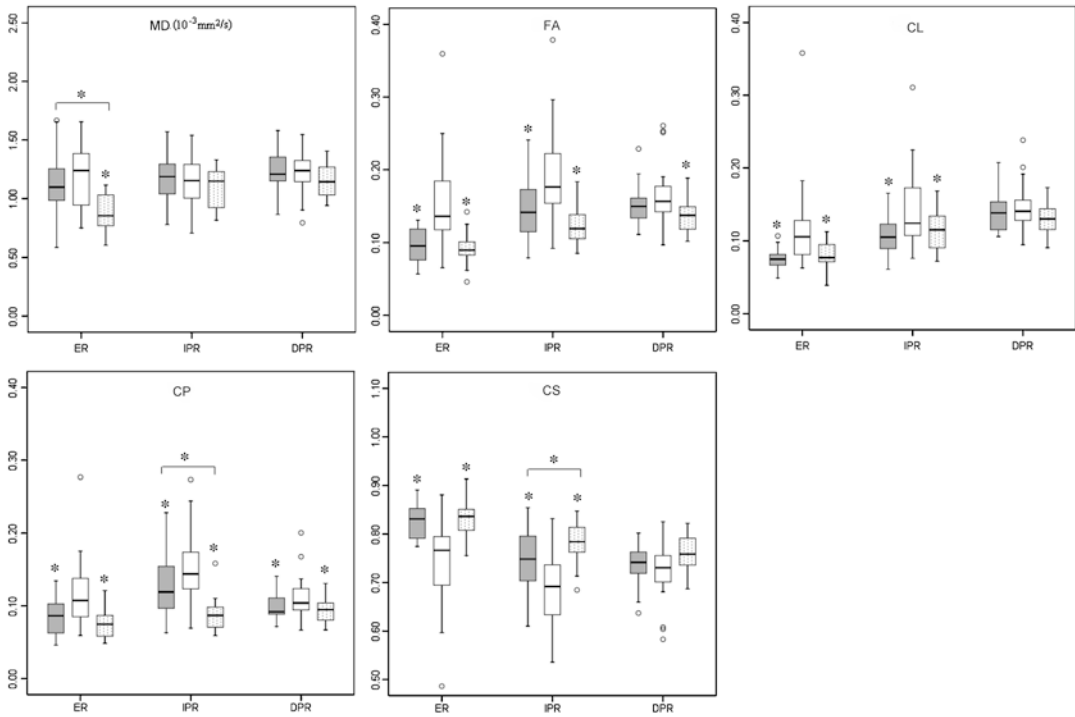


Fig. 2.5 Box plots of diffusion characteristics in brain metastases (gray), glioblastomas (white), and primary cerebral lymphomas (PCLs, dotted). The solid line inside the box represents the median value, while the edges represent the 25th and 75th percentiles. Straight line (bars) on each box indicates the range of data distribution. Circles represent outliers (values more than 1.5 box length from the 75th/25th percentile). *Above gray or dotted box

indicates significant difference ($p < 0.05$) for glioblastomas vs. metastases or glioblastomas vs. PCLs, respectively. *Above a horizontal line between gray and dotted boxes indicates significant difference ($p < 0.05$) between metastases and PCLs. ER: enhancing region. IPR: immediate peritumoral region. DPR: distant peritumoral region. Reprinted and modified with permission from Wang et al. [21]

Histogram Analysis of DTI

Many of the challenges in use of DTI for characterizing brain tumors stem from the heterogeneity within or across tumor types. Standard ROI summary statistics of mean or median, however, do not address tumor spatial heterogeneity. The degree of tumor heterogeneity typically correlates with the tumor grade. The higher the heterogeneity, the more malignant the tumor is. Use of histogram for studying distributions of different parameters provides a better assessment of tissue heterogeneity, and is thus more objective and may result in higher reproducibility.

Histogram analysis of perfusion parameters has been successfully used in brain tumor classification [60–62]. Histogram-derived parameters

varied in different studies, including mean, variance, peak height position, peak width, skewness, and kurtosis. But histogram analysis in DTI has not been well documented. Tozer et al. [63] reported that low-grade oligodendrogliomas are more homogeneous and showed lower MD compared with low-grade astrocytomas. Jakab et al. [61] recently reported that using histogram bins from FA, axial diffusivity, DWI, and B0 maps can differentiate low-grade from high-grade gliomas. MD histogram analysis has also been used to predict response to treatment in patients with recurrent GBM [64]. Minimum MD values have been found to be prognostic of outcomes in gliomas [65]. Recently, Wang et al. [66] have utilized histogram to quantify the diffusion data in meningiomas. Four histogram parameters, mean,

variance, skewness, and kurtosis, were extracted from the enhancing part of the tumor. Their result indicated that histogram analysis of eigenvalue skewness can help differentiate atypical from typical meningiomas. Among typical meningiomas, histogram analysis of tensor shape measurements can distinguish fibroblastic from other subtype meningiomas [66].

Combined DTI Metrics for Classification

DTI provides a number of parameters about the shape, magnitude, and degree of diffusion anisotropy, which may be used to differentiate different tumor types. However, these parameters, by themselves individually, have a limited role in tumor classification. Wang et al. have previously reported that the single best predictor for differentiation between glioblastomas and brain metastases is FA, with a sensitivity of 89 %, specificity of 80 %, and AUC of 0.90 [22]. Accurate characterization of complicated tissue, such as a tumor, may require

two or more imaging parameters. To date, only a limited number of studies have investigated the role of DTI parameters in combination for tumor classification. One study suggested that a combination of minimum MDs and difference of MD facilitates more accurate grading of astrocytomas than either parameter measured individually [7], whereas another study indicated that a combination of mean FA and maximum FA improves the diagnostic accuracy of nonenhancing gliomas [26]. Wang et al. have previously reported that a multivariate logistic regression analysis can determine an optimal combination of DTI parameters to differentiate glioblastomas from brain metastases and primary cerebral lymphomas [21, 22]. Their results indicated that the best model to distinguish glioblastomas from non-glioblastomas consisted of MD, CS (or FA) from the enhancing region, and rCBV from the immediate peritumoral region, resulting in an AUC of 0.938. The best predictor to differentiate primary cerebral lymphomas from brain metastases comprised MD from the enhancing region and CP from the immediate peritumoral region with AUC of 0.909 (Fig. 2.6).

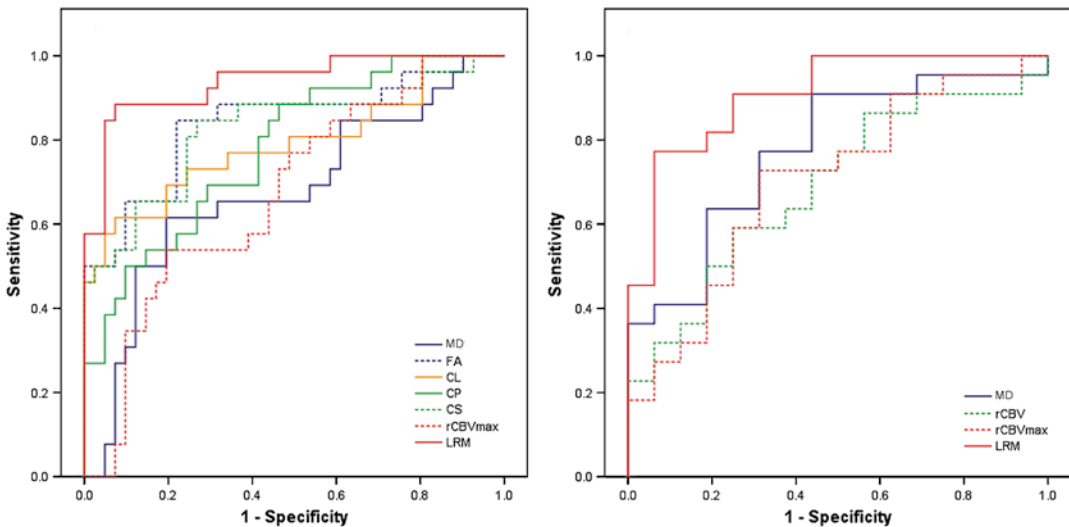


Fig. 2.6 Receiver operating characteristic (ROC) curves of the imaging parameters with high predictive power from the enhancing part as well as the logistic regression model (LRM) for differentiation between glioblastomas and non-glioblastomas (**a**), brain metastases, and primary cerebral lymphomas (PCLs, **b**). LRM of MD, CS from ER, and rCBV from the IPR was the best predictor for

differentiation of glioblastomas from non-glioblastomas with area under the curve (AUC) of 0.938 (**a**), whereas combination of MD from the ER and CP from the IPR was the best model for distinguishing lymphomas from metastases with AUC of 0.909 (**b**). Reprinted and modified with permission from Wang et al. [21]

Conclusion

As reviewed in this chapter, a number of studies have demonstrated the high potential of DTI as a promising tool to study microstructural differences among different tumor types and grades. DTI metrics, such as MD, FA, CL, CP, and CS, can be used individually or in combination for brain tumor characterization. Further investigations on a larger patient population and histological validation will be necessary to determine the underlying tissue properties associated with DTI measures and to improve the robustness of these parameters in differentiating tumor types. With the recent development of new techniques, such as diffusion kurtosis imaging (DKI) and diffusion spectrum imaging (DSI), the clinical significance of diffusion imaging in brain tumor will be further established and acknowledged.

References

- Central Brain Tumor Registry of the United States. Statistical report: primary brain and central nervous system tumors diagnosed in the United States, 2004–2007. Central Brain Tumor Registry of the United States. 2011.
- Chenevert TL, Ross BD. Diffusion imaging for therapy response assessment of brain tumor. *Neuroimaging Clin N Am*. 2009;19(4):559–71.
- Louis DN, Ohgaki H, Wiestler OD, et al. The 2007 WHO classification of tumours of the central nervous system. *Acta Neuropathol*. 2007;114(2):97–109.
- Batchelor T, Loeffler JS. Primary CNS lymphoma. *J Clin Oncol*. 2006;24(8):1281–8.
- Giese A, Westphal M. Treatment of malignant glioma: a problem beyond the margins of resection. *J Cancer Res Clin Oncol*. 2001;127(4):217–25.
- Soffietti R, Ruda R, Mutani R. Management of brain metastases. *J Neurol*. 2002;249(10):1357–69.
- Murakami R, Hirai T, Sugahara T, et al. Grading astrocytic tumors by using apparent diffusion coefficient parameters: superiority of a one- versus two-parameter pilot method. *Radiology*. 2009;251(3):838–45.
- Yamasaki F, Kurisu K, Satoh K, et al. Apparent diffusion coefficient of human brain tumors at MR imaging. *Radiology*. 2005;235(3):985–91.
- Stadlbauer A, Ganslandt O, Buslei R, et al. Gliomas: histopathologic evaluation of changes in directionality and magnitude of water diffusion at diffusion-tensor MR imaging. *Radiology*. 2006;240(3):803–10.
- Al-Okaili RN, Krejza J, Woo JH, et al. Intraaxial brain masses: MR imaging-based diagnostic strategy—initial experience. *Radiology*. 2007;243(2):539–50.
- Melhem ER, Mori S, Mukundan G, Kraut MA, Pomper MG, van Zijl PC. Diffusion tensor MR imaging of the brain and white matter tractography. *AJR Am J Roentgenol*. 2002;178(1):3–16.
- Beaulieu C. The basis of anisotropic water diffusion in the nervous system—a technical review. *NMR Biomed*. 2002;15(7–8):435–55.
- Basser PJ, Pierpaoli C. Microstructural and physiological features of tissues elucidated by quantitative-diffusion-tensor MRI. *J Magn Reson B*. 1996;111(3):209–19.
- Westin CF, Maier SE, Mamata H, Nabavi A, Jolesz FA, Kikinis R. Processing and visualization for diffusion tensor MRI. *Med Image Anal*. 2002;6(2):93–108.
- Alexander AL, Hasan K, Kindlmann G, Parker DL, Tsuruda JS. A geometric analysis of diffusion tensor measurements of the human brain. *Magn Reson Med*. 2000;44(2):283–91.
- Chenevert TL, Sundgren PC, Ross BD. Diffusion imaging: insight to cell status and cytoarchitecture. *Neuroimaging Clin N Am*. 2006;16(4):619–32. viii-ix.
- Guo AC, Cummings TJ, Dash RC, Provenzale JM. Lymphomas and high-grade astrocytomas: comparison of water diffusibility and histologic characteristics. *Radiology*. 2002;224(1):177–83.
- Nagar VA, Ye JR, Ng WH, et al. Diffusion-weighted MR imaging: diagnosing atypical or malignant meningiomas and detecting tumor dedifferentiation. *AJNR Am J Neuroradiol*. 2008;29(6):1147–52.
- Toh CH, Castillo M, Wong AM, et al. Differentiation between classic and atypical meningiomas with use of diffusion tensor imaging. *AJNR Am J Neuroradiol*. 2008;29(9):1630–5.
- Lu S, Ahn D, Johnson G, Law M, Zagzag D, Grossman RI. Diffusion-tensor MR imaging of intracranial neoplasia and associated peritumoral edema: introduction of the tumor infiltration index. *Radiology*. 2004;232(1):221–8.
- Wang S, Kim S, Chawla S, et al. Differentiation between glioblastomas, solitary brain metastases, and primary cerebral lymphomas using diffusion tensor and dynamic susceptibility contrast-enhanced MR imaging. *AJNR Am J Neuroradiol*. 2011;32(3):507–14.
- Wang S, Kim S, Chawla S, et al. Differentiation between glioblastomas and solitary brain metastases using diffusion tensor imaging. *Neuroimage*. 2009;44(3):653–60.
- Lu S, Ahn D, Johnson G, Cha S. Peritumoral diffusion tensor imaging of high-grade gliomas and metastatic brain tumors. *AJNR Am J Neuroradiol*. 2003;24(5):937–41.
- Morita K, Matsuzawa H, Fujii Y, Tanaka R, Kwee IL, Nakada T. Diffusion tensor analysis of peritumoral edema using lambda chart analysis indicative of the heterogeneity of the microstructure within edema. *J Neurosurg*. 2005;102(2):336–41.

25. Lee EJ, Lee SK, Agid R, Bae JM, Keller A, Terbrugge K. Preoperative grading of presumptive low-grade astrocytomas on MR imaging: diagnostic value of minimum apparent diffusion coefficient. *AJNR Am J Neuroradiol.* 2008;29(10):1872–7.
26. Liu X, Tian W, Kolar B, et al. MR diffusion tensor and perfusion-weighted imaging in preoperative grading of supratentorial nonenhancing gliomas. *Neuro Oncol.* 2011;13(4):447–55.
27. Calli C, Kitis O, Yuntun N, Yurtseven T, Islekel S, Akalin T. Perfusion and diffusion MR imaging in enhancing malignant cerebral tumors. *Eur J Radiol.* 2006;58(3):394–403.
28. Oh J, Cha S, Aiken AH, et al. Quantitative apparent diffusion coefficients and T2 relaxation times in characterizing contrast enhancing brain tumors and regions of peritumoral edema. *J Magn Reson Imaging.* 2005;21(6):701–8.
29. Jolapara M, Kesavadas C, Radhakrishnan VV, et al. Role of diffusion tensor imaging in differentiating subtypes of meningiomas. *J Neuroradiol.* 2010;37(5):277–83.
30. Zamecnik J. The extracellular space and matrix of gliomas. *Acta Neuropathol.* 2005;110(5):435–42.
31. Vargova L, Homola A, Zamecnik J, Tichy M, Benes V, Sykova E. Diffusion parameters of the extracellular space in human gliomas. *Glia.* 2003;42(1):77–88.
32. McConville P, Hambardzumyan D, Moody JB, et al. Magnetic resonance imaging determination of tumor grade and early response to temozolomide in a genetically engineered mouse model of glioma. *Clin Cancer Res.* 2007;13(10):2897–904.
33. Moffat BA, Chenevert TL, Lawrence TS, et al. Functional diffusion map: a noninvasive MRI biomarker for early stratification of clinical brain tumor response. *Proc Natl Acad Sci U S A.* 2005;102(15):5524–9.
34. Padhani AR, Liu G, Koh DM, et al. Diffusion-weighted magnetic resonance imaging as a cancer biomarker: consensus and recommendations. *Neoplasia.* 2009;11(2):102–25.
35. Wang S, Wolf RL, Woo JH, et al. Actinomycotic brain infection: registered diffusion, perfusion MR imaging and MR spectroscopy. *Neuroradiology.* 2006;48(5):346–50.
36. Beppu T, Inoue T, Shibata Y, et al. Measurement of fractional anisotropy using diffusion tensor MRI in supratentorial astrocytic tumors. *J Neurooncol.* 2003;63(2):109–16.
37. Beppu T, Inoue T, Shibata Y, et al. Fractional anisotropy value by diffusion tensor magnetic resonance imaging as a predictor of cell density and proliferation activity of glioblastomas. *Surg Neurol.* 2005;63(1):56–61. discussion 61.
38. Haris M, Gupta RK, Husain N, Hasan KM, Husain M, Narayana PA. Measurement of DTI metrics in hemorrhagic brain lesions: possible implication in MRI interpretation. *J Magn Reson Imaging.* 2006;24(6):1259–68.
39. Kinoshita M, Hashimoto N, Goto T, et al. Fractional anisotropy and tumor cell density of the tumor core show positive correlation in diffusion tensor magnetic resonance imaging of malignant brain tumors. *NeuroImage.* 2008;43:29–35.
40. Toh CH, Castillo M, Wong AM, et al. Primary cerebral lymphoma and glioblastoma multiforme: differences in diffusion characteristics evaluated with diffusion tensor imaging. *AJNR Am J Neuroradiol.* 2008;29(3):471–5.
41. Inoue T, Ogasawara K, Beppu T, Ogawa A, Kabasawa H. Diffusion tensor imaging for preoperative evaluation of tumor grade in gliomas. *Clin Neurol Neurosurg.* 2005;107(3):174–80.
42. Wang W, Steward CE, Desmond PM. Diffusion tensor imaging in glioblastoma multiforme and brain metastases: the role of p, q, L, and fractional anisotropy. *AJNR Am J Neuroradiol.* 2009;30(1):203–8.
43. Reiche W, Schuchardt V, Hagen T, Il'yasov KA, Billmann P, Weber J. Differential diagnosis of intracranial ring enhancing cystic mass lesions—role of diffusion-weighted imaging (DWI) and diffusion-tensor imaging (DTI). *Clin Neurol Neurosurg.* 2010;112(3):218–25.
44. Koeller KK, Smirniotopoulos JG, Jones RV. Primary central nervous system lymphoma: radiologic-pathologic correlation. *Radiographics.* 1997;17(6):1497–526.
45. Rees JH, Smirniotopoulos JG, Jones RV, Wong K. Glioblastoma multiforme: radiologic-pathologic correlation. *Radiographics.* 1996;16(6):1413–38. quiz 1462–1413.
46. Zhang M, Olsson Y. Hematogenous metastases of the human brain—characteristics of peritumoral brain changes: a review. *J Neurooncol.* 1997;35(1):81–9.
47. Zhang S, Bastin ME, Laidlaw DH, Sinha S, Armitage PA, Deisboeck TS. Visualization and analysis of white matter structural asymmetry in diffusion tensor MRI data. *Magn Reson Med.* 2004;51(1):140–7.
48. Kim S, Pickup S, Hsu O, Poptani H. Diffusion tensor MRI in rat models of invasive and well-demarcated brain tumors. *NMR Biomed.* 2008;21(3):208–16.
49. Lope-Piedrafita S, Garcia-Martin ML, Galons JP, Gillies RJ, Trouard TP. Longitudinal diffusion tensor imaging in a rat brain glioma model. *NMR Biomed.* 2008;21(8):799–808.
50. Zhang J, van Zijl PC, Laterra J, et al. Unique patterns of diffusion directionality in rat brain tumors revealed by high-resolution diffusion tensor MRI. *Magn Reson Med.* 2007;58(3):454–62.
51. Kashimura H, Inoue T, Ogasawara K, et al. Prediction of meningioma consistency using fractional anisotropy value measured by magnetic resonance imaging. *J Neurosurg.* 2007;107(4):784–7.
52. Tropine A, Dellani PD, Glaser M, et al. Differentiation of fibroblastic meningiomas from other benign subtypes using diffusion tensor imaging. *J Magn Reson Imaging.* 2007;25(4):703–8.
53. Kumar M, Gupta RK, Nath K, et al. Can we differentiate true white matter fibers from pseudofibers inside a brain abscess cavity using geometrical diffusion

- tensor imaging metrics? *NMR Biomed.* 2007;21(6): 581–8.
54. Santhosh K, Thomas B, Radhakrishnan VV, et al. Diffusion tensor and tensor metrics imaging in intracranial epidermoid cysts. *J Magn Reson Imaging.* 2009;29(4):967–70.
 55. Gupta RK, Haris M, Husain N, Saksena S, Husain M, Rathore RK. DTI derived indices correlate with immunohistochemistry obtained matrix metalloproteinase (MMP-9) expression in cellular fraction of brain tuberculoma. *J Neurol Sci.* 2008;275(1–2):78–85.
 56. Lee EJ, Lee EJ, Lee EJ, Terbrugge K, Mikulis D, et al. Diagnostic value of peritumoral minimum apparent diffusion coefficient for differentiation of glioblastoma multiforme from solitary metastatic lesions. *AJR Am J Roentgenol.* 2011;196(1):71–6.
 57. van Westen D, Latt J, Englund E, Brockstedt S, Larsson EM. Tumor extension in high-grade gliomas assessed with diffusion magnetic resonance imaging: values and lesion-to-brain ratios of apparent diffusion coefficient and fractional anisotropy. *Acta Radiol.* 2006;47(3):311–9.
 58. Kinoshita M, Goto T, Okita Y, et al. Diffusion tensor-based tumor infiltration index cannot discriminate vasogenic edema from tumor-infiltrated edema. *J Neurooncol.* 2010;96(3):409–15.
 59. Law M, Cha S, Knopp EA, Johnson G, Arnett J, Litt AW. High-grade gliomas and solitary metastases: differentiation by using perfusion and proton spectroscopic MR imaging. *Radiology.* 2002;222(3):715–21.
 60. Emblem KE, Nedregaard B, Nome T, et al. Glioma grading by using histogram analysis of blood volume heterogeneity from MR-derived cerebral blood volume maps. *Radiology.* 2008;247(3):808–17.
 61. Jakab A, Molnar P, Emri M, Berenyi E. Glioma grade assessment by using histogram analysis of diffusion tensor imaging-derived maps. *Neuroradiology.* 2011; 53(7):483–91. Epub 2010 Sep 21.
 62. Kim HS, Kim JH, Kim SH, Cho KG, Kim SY. Posttreatment high-grade glioma: usefulness of peak height position with semiquantitative MR perfusion histogram analysis in an entire contrast-enhanced lesion for predicting volume fraction of recurrence. *Radiology.* 2010;256(3):906–15.
 63. Tozer DJ, Jager HR, Danchaivijitr N, et al. Apparent diffusion coefficient histograms may predict low-grade glioma subtype. *NMR Biomed.* 2007;20(1): 49–57.
 64. Pope WB, Kim HJ, Huo J, et al. Recurrent glioblastoma multiforme: ADC histogram analysis predicts response to bevacizumab treatment. *Radiology.* 2009; 252(1):182–9.
 65. Pope WB, Lai A, Mehta R, et al. Apparent diffusion coefficient histogram analysis stratifies progression-free survival in newly diagnosed bevacizumab-treated glioblastoma. *AJNR Am J Neuroradiol.* 2011;32(5): 882–9.
 66. Wang S, Kim S, Zhang Y, et al. Determination of grade and subtype of meningiomas by using histogram analysis of diffusion-tensor Imaging metrics. *Radiology.* 2012;262:584–92.

Functional Brain Tumor Imaging

Pillai, J.J. (Ed.)

2014, XIII, 250 p. 125 illus., 101 illus. in color.,

Hardcover

ISBN: 978-1-4419-5857-0